AGU PUBLICATIONS

Geophysical Research Letters

RESEARCH LETTER

10.1002/2016GL070090

Key Points:
- The solar wind-magnetosphere interaction generates *DP* 2 current fluctuation
- The *DP* 2 current fluctuations penetrate to the equator and cause the equatorial electrodynamics to fluctuate
- It also causes the equatorial density to fluctuate which might affect the communication and navigation systems

Correspondence to:
E. Yizengaw,
Kassie@bc.edu

Citation:
Yizengaw, E., M. B. Moldwin, E. Zesta, M. Magoun, R. Pradipta, C. M. Biouele, A. B. Rabiu, O. K. Obrou, Z. Bamba, and E. R. de Paula (2016), Response of the equatorial ionosphere to the geomagnetic *DP* 2 current system, *Geophys. Res. Lett.*, *43*, 7364–7372, doi:10.1002/2016GL070090.

Received 19 MAY 2016
Accepted 8 JUL 2016
Accepted article online 12 JUL 2016
Published online 25 JUL 2016

Response of the equatorial ionosphere to the geomagnetic *DP* 2 current system

E. Yizengaw[1], M. B. Moldwin[2], E. Zesta[3], M. Magoun[1], R. Pradipta[1], C. M. Biouele[4], A. B. Rabiu[5], O. K. Obrou[6], Z. Bamba[7], and E. R. de Paula[8]

[1]Institute for Scientific Research, Boston College, Boston, Massachusetts, USA, [2]Department of Climate, Space Sciences, and Engineering, University of Michigan, Ann Arbor, Michigan, USA, [3]NASA Goddard Space Flight Center, Greenbelt, Maryland, USA, [4]Department of Physics, University of Yaoundé I, Yaoundé, Cameroon, [5]National Space Research and Development Agency, Abuja, Nigeria, [6]Laboratorie de physique de l'atmosphère, Université Félix Houphouët-Boigny FHB, Abidjan, Cote d'Ivoire, [7]Centre de Recherche Scientifique de Conakry Rogbanè, Conakry, Guinea, [8]Instituto Nacional de Pesquisas Espaciais, São José dos Campos, Brazil

Abstract The response of equatorial ionosphere to the magnetospheric origin *DP* 2 current system fluctuations is examined using ground-based multiinstrument observations. The interaction between the solar wind and magnetosphere generates a convection electric field that can penetrate to the ionosphere and cause the *DP* 2 current system. The quasiperiodic *DP* 2 current system, which fluctuates coherently with fluctuations of the interplanetary magnetic field (IMF) B_z, penetrates nearly instantaneously to the dayside equatorial region at all longitudes and modulates the electrodynamics that governs the equatorial density distributions. In this paper, using magnetometers at high and equatorial latitudes, we demonstrate that the quasiperiodic *DP* 2 current system penetrates to the equator and causes the dayside equatorial electrojet (EEJ) and the independently measured ionospheric drift velocity to fluctuate coherently with the high-latitude *DP* 2 current as well as with the IMF B_z component. At the same time, radar observations show that the ionospheric density layers move up and down, causing the density to fluctuate up and down coherently with the EEJ and IMF B_z.

1. Introduction

It is well known that geomagnetic disturbances in the high-latitude region consist of two morphologically distinct current systems (*DP* 1 and *DP* 2 currents) that are associated directly with magnetospheric convection. The *DP* 1 (disturbance polar of the first type) current (the substorm westward electrojet) disturbance, which is associated with the substorm expansion phase [*Claver and Kamide*, 1985], is characterized by a strong intensification of the westward auroral electrojet and cause the formation of magnetic bays in the auroral region [*Nishida*, 1968]. While the *DP* 1 current system is localized in the near-local midnight region, the polar region *DP* 2 (disturbance polar of the second type) current disturbances are global and characterized by quasiperiodic magnetic fluctuations with a timescale of 30 min to several hours [e.g., *Nishida*, 1968; *Kikuchi et al.*, 1996, 2000, 2008]. Unlike the *DP* 1 current system, the *DP* 2 current system can occur during both quiet and disturbed times and its impact can be detected at all latitudes with different magnitudes [*Claver and Kamide*, 1985]. All of these phenomenological characteristics have been determined primarily from ground magnetometer observations over many decades.

Understanding the formation of the quasiperiodic ionospheric current systems is very important to our comprehension of the solar wind magnetosphere-ionosphere coupling process and its impact on the equatorial density distribution. In the presence of interplanetary magnetic field, the interaction between solar wind and magnetosphere produces a dawn-to-dusk convection electric field ($E_y = -(V_x \times B_z)$). This electric field can then penetrate into the magnetosphere when the IMF B_z turns south and drives *DP* 2 current system [*Nishida*, 1968]. The equivalent *DP* 2 current fluctuation, which consists of twin current vortices at high latitudes and zonal current component at low latitudes, then extends all over the Earth from the pole to the equator [e.g., *Nishida*, 1968]. Since the solar wind speed is relatively steady compared to IMF B_z, the time fluctuation of the convection electric field may be directly proportional to the variation of IMF B_z instead of solar wind speed. Thus, the time fluctuation of the *DP* 2 current systems both at high-latitude and equatorial regions is primarily controlled by the IMF B_z fluctuation. *Nishida* [1968], using the combined data from Explorer 18 (IMP 1) spacecraft and ground-based magnetometers,

Table 1. List of Instruments Used for This Study

Stations	Geographic Coordinate Latitude (°N)	Geographic Coordinate Longitude (°E)	Geomagnetic Coordinate Latitude (°N)	Geomagnetic Coordinate Longitude (°E)	Operated Under the Umbrella of
List of magnetometers					
Abidjan	4.60	−6.64	−6.0	65.82	AMBER
Abuja	10.5	7.55	−0.55	79.63	AMBER
Belem	−1.45	−48.5	−1.05	25.34	AMBER
Conakry	10.5	−13.71	−0.46	60.37	AMBER
Petrolina	−9.5	−40.5	−6.95	30.21	AMBER
Yaoundé	3.78	11.52	−5.30	83.12	AMBER
Jicamarca	−11.95	−76.88	0.61	−5.40	JICAMARCA
Piura	−5.17	−80.64	6.84	−9.40	JICAMARCA
Alta Floresta	−9.87	−56.1	−0.75	15.18	LISN
Cuiaba	−15.56	−56.1	−5.85	13.80	LISN
Leticia	−4.2	−69.9	8.18	2.00	LISN
Huancayo	−12.05	−75.33	0.63	−3.89	INTERMAGNET
Iqaluit	63.75	−68.52	73.21	14.91	INTERMAGNET
King Edward Point	−54.28	−36.49	−43.64	24.75	INTERMAGNET
Mbour	14.38	−16.97	2.06	58.24	INTERMAGNET
Narsarsuaq	61.16	−45.44	66.47	43.91	INTERMAGNET
Qaanaaq (Thule)	77.47	−69.23	85.63	33.34	INTERMAGNET
GPS receivers					
Jicamarca	−11.95	−76.88	−0.87	16.35	LISN
Ionosonde station					
Boa Vista	2.8	−60.7	12.55	13.47	GIRO

demonstrated that the *DP* 2 currents both at high and equatorial latitudes fluctuate coherently with IMF B_z. Therefore, the presence of the *DP* 2 current fluctuation at the equator is the direct result of the quasi-periodic interplanetary electric field that penetrates into the magnetosphere and down to the equatorial ionosphere through the TM0 (zero order transverse magnetic) mode waves in the Earth-ionosphere wave-guide [*Kikuchi et al.*, 2008].

When the IMF B_z turns south, the interaction between the geomagnetic field and IMF produces two reconnection locations, at the dayside (sunwardside) and nightside (tailside) [*Nishida*, 1968]. Although it is the source of many important processes, such as energization of charged particles and expansion of substorm (or formation of *DP* 1 current system), the field-aligned currents that originate from nightside reconnection may not be the cause for the *DP* 2 current system, because the transit time of the event from the tailside reconnection region (away from the ground by tens to few hundred R_E) to the ground is much greater than the *DP* 2 fluctuation time. This implies that field-aligned currents that originate from dayside reconnection drive the *DP* 2 current system. However, the time-varying interplanetary electric field can penetrate into the magnetosphere if the electric conductivity along the field lines on the magnetopause is low. *Parker* [1967] suggested that the magnetopause surface conductivity decreases in the region where the angle between solar wind velocity and the geomagnetic field decreases. Since the conductivity along the field lines on frontside of the magnetopause is believed to be high, the time-varying electric field cannot penetrate to the magnetosphere from the frontside of the magnetopause, but instead, it penetrates from around the morning-evening sector of the magnetopause where field-aligned electric conductivity is low and the finite potential difference is applied across the magnetopause [*Nishida*, 1968].

Although there have been many studies of the *DP* 2 current system and its impact on magnetic fluctuations in the equatorial region [e.g., *Nishida*, 1968; *Clauer and Kamide*, 1985; *Kikuchi et al.*, 1996, 2000, 2008; *Trivedi et al.*, 2002], there are still several important questions that remain unresolved. One of these major questions is what kind of impact can the *DP* 2 current system impose on the equatorial ionospheric density distribution? This study for the first time shows the response of the ionospheric density distribution to the fluctuation of the *DP* 2 current system at the equator that can modulate the equatorial electrodynamics to fluctuate with the same periodicity as the *DP* 2 current system or as IMF B_z.

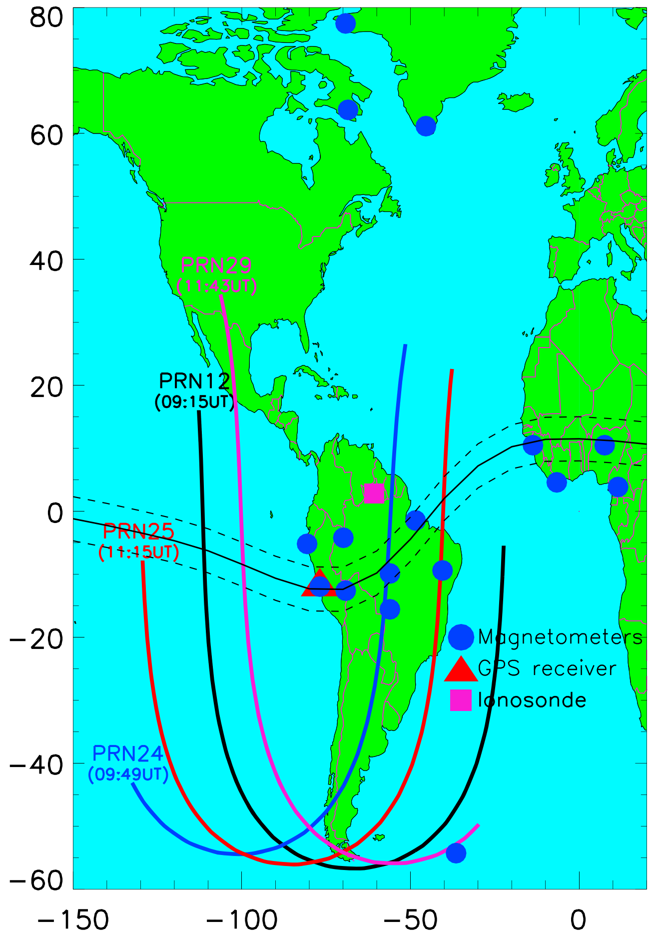

Figure 1. The geographic locations of the ground-based instruments that are used in this analysis.

2. Data Analysis

For this study, we used data from ground-based magnetometers that are located at auroral and equatorial latitudes to estimate the *DP* 2 currents and the EEJ that occurred on 16 February 2016 and 2 May 2010. The detailed description of the technique that we use to identify the *DP* 2 current systems and EEJ from the magnetometer observations can be found in, e.g., *Kikuchi et al.* [1996], *Anderson et al.* [2004], *Yizengaw et al.* [2014], and the reference therein, respectively. The magnetometers we use for this study are operated under the umbrella of African Meridian *B*-field Education and Research (AMBER) [*Yizengaw and Moldwin*, 2009], INTERMAGNET [*Love and Chulliat*, 2003], and the Low Latitude Ionospheric Sensor Network (LISN) [*Valladares and Chau*, 2012] projects. The geographic and geomagnetic coordinates of the magnetometers used are listed in Table 1.

Similarly, to estimate the response of the ionosphere to the *DP* 2 current system dynamics, we use vertical total electron content (VTEC) measurements from GPS receivers operated under the LISN networks and ionosonde observations from the Global Ionospheric Radio Observatory (GIRO) network [*Reinisch and Galkin*, 2011]. Figure 1 shows the location of all magnetometers, GPS receivers, and ionosonde stations that are used in this study. The solid and dashed curves depict the location of the magnetic equator and the region of EEJ (i.e., ±3.5° magnetic latitudes), respectively. The colored solid curves at the bottom left corner of Figure 1 show the ground tracks of the GPS satellites, of which the pseudo-random noise (PRN) and the starting time of each pass are also shown at the beginning of each pass.

3. Observations

Figure 2 (first panel) shows the characteristics of solar wind parameters, IMF B_z (black curve), and the dawn-to-dusk interplanetary electric field (IEF) (red curve) observed on 16 February 2016. Both of them show strong quasiperiodic fluctuations with a dominant periodicity of around 45 min. Although the solar wind parameters show periodic fluctuations, there was no significant magnetic storm activity. *Dst* index was quiet with $Dst > -60$ nT, but *Kp* index indicates the presence of a moderate storm with $Kp = 5$, which is not surprising as the *DP* 2 current fluctuation can also occur during geomagnetically quiet periods [*Claver and Kamide*, 1985].

Figure 2 (second panel) depicts the *x*-component (approximately north-south direction) magnetic field variations obtained from four magnetometers located at high and auroral latitudes. Different colors represent different stations where the stations' codes and geomagnetic latitudes are shown at the rightside. In order to maintain the magnetic field fluctuation within the same range limit, we multiplied the magnetic field fluctuation with the correspondingly colored numbers shown inside each panel.

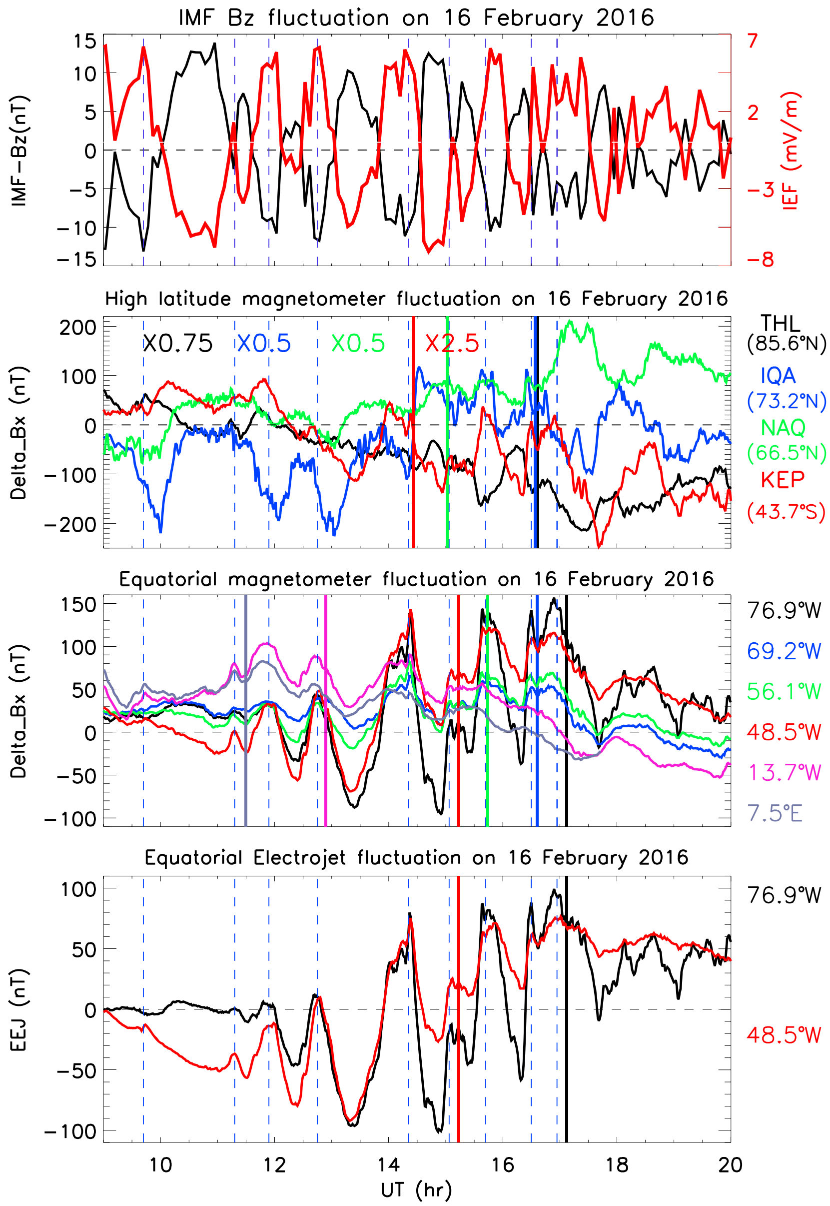

Figure 2. (top to bottom) IMF B_z (black curve) and IEF (red curve), the *x* component of four high-latitude magnetometers, *x*-component magnetic field variation from six equatorial magnetometers, and EEJ estimated at different meridians.

Figure 2 (third panel) indicates the *x*-component magnetic field fluctuations observed in the equatorial region, within ±8° geomagnetic latitude, using stations located at different longitudes. The different colors represent different longitudes (noted on the rightside of the panel), expanding from west American to west African regions. All of them exhibit coherent fluctuation with IMF B_z, in which the fluctuations are stronger around local noon when solar UV irradiation is stronger, and thus, ionosphereic conductance enhanced. Finally, the EEJ, which is directly proportional to the equatorial vertical drift [e.g., *Anderson et al.*, 2004] that governs the equatorial ionospheric density distribution, that was calculated at two different longitudes, show identical fluctuation (see Figure 2, fourth panel) with the same periodicity of IMF B_z fluctuations. The magnitude and direction of EEJ are calculated using pairs of ground magnetometers located approximately at the dip equator and off the geomagnetic equator (~6–9° geomagnetic) latitudes [*Anderson et al.*, 2004; *Yizengaw et al.*, 2014]. The vertical solid lines, shown from second to fourth panels, depict the local noon for the corresponding stations. The vertical dashed lines shown in all panels indicate the time

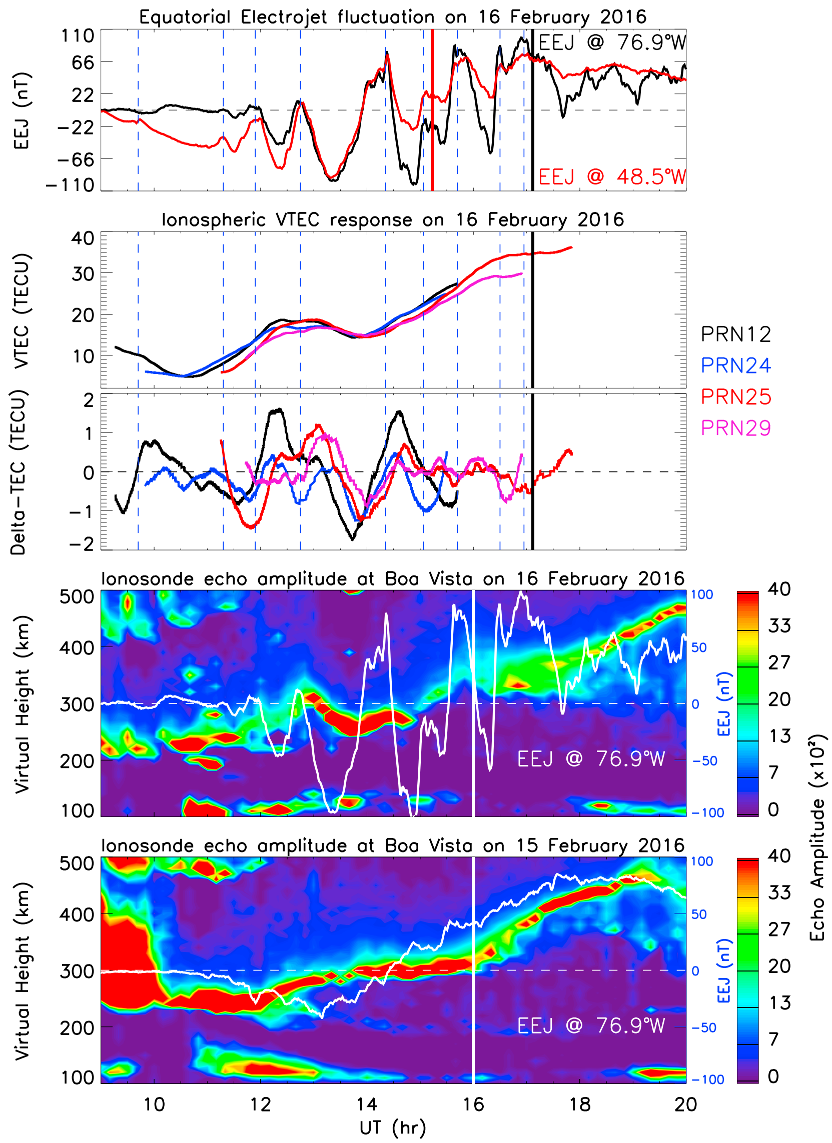

Figure 3. (first panel) EEJ estimated at two different longitudes. (second and third panels) VTEC segments from four different PRN and the corresponding filtered VTEC. (fourth and fifth panels) The range-time-intensity-style plot of ionospheric echoes received from ionosonde located at Boa Vista, and the overplotted white curves depict the EEJ during the corresponding days given at the top of each panel.

coincidence of the IMF B_z minimum point (or the IEF peaks), the magnetic variation peaks at different latitudes and longitudes, and the EEJ peaks.

Figure 3 presents the response of the ionosphere for the quasiperiodic fluctuations of the solar wind parameters and the EEJ measurements. Figure 3 (first panel) shows the EEJ at the western and easternside of South America, which is the same as in Figure 2, fourth panel. The vertical solid lines indicate the local noon for the correspondingly colored EEJs. Figure 3 (second panel) shows the VTEC obtained by the GPS receiver located at Jicamarca on 16 February 2016. The corresponding filtered VTEC (by subtracting the sixth-order polynomial fit from the actual VTEC) shows clear VTEC fluctuations that exhibit good correlation with EEJ fluctuation. Different colors represent the VTEC segment obtained by tracking different GPS satellites, in which the PRN numbers of each satellite are given at the rightside. The ground tracks of each satellite are shown, as line curves, in Figure 1, which are correspondingly colored as the VTEC curves shown in the second and third panels of Figure 3. The contour in Figure 3 (fourth and fifth panels) depicts the aggregate number of

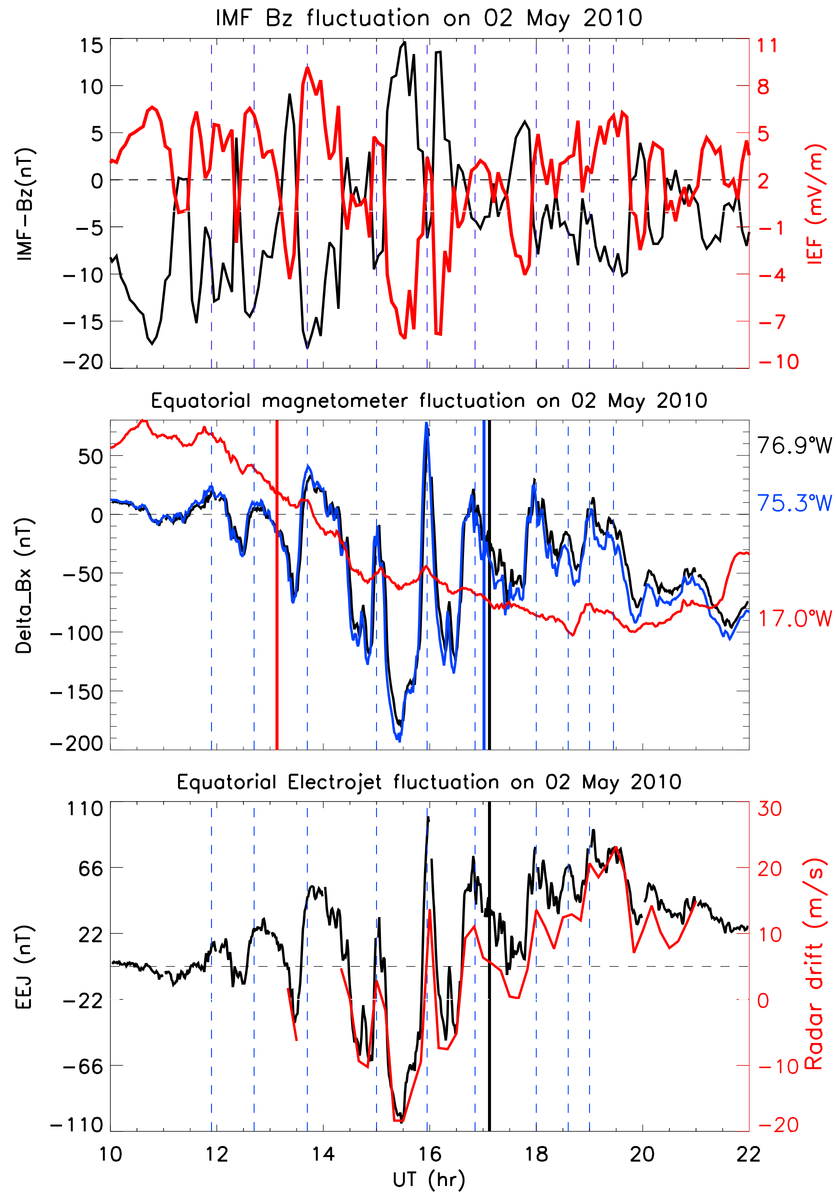

Figure 4. As for Figure 2 but for a different day that is given at the top of the panels.

return echoes recorded by the digisonde at Boa Vista on 15 and 16 February 2016 (as a function of height and time). Ionograms were recorded once every 15 min, and the return echoes are summed over all sounding frequencies. The color represents the level of total echo amplitudes at any given height and time, and the white curve indicates the EEJ estimated from the nearby pair of magnetometers located at the 76.9°W meridian. The height of maximum total echo amplitude often coincides with h_mF_2, especially in terms of their time rate of change. Thus, we used the height of maximum total echo amplitude fluctuations to track the up and down movement of the ionospheric *F* layer, which is a good indicator how the ionospheric density fluctuates up and down in the presence of *DP* 2 current systems.

Figure 4 (top) shows another example, specifically the periodic IMF B_z (black curve) fluctuations and the respective IEF (red curve) observed on 2 May 2010. Figure 4 (middle) presents the magnetic variation observed at three equatorial stations located at different longitudes, which are noted on the right side, and the fluctuations are stronger around local noon. The solid vertical lines depict local noon of the corresponding stations. Unlike the 16 February 2016 event, the Jicamarca radar was running on Jicamarca

Unattended Long-term investigations of the Ionosphere and Atmosphere (JULIA) mode and provided ionospheric vertical irregularity drifts during the 2 May 2010 event. The irregularity vertical drift (red curve) is overplotted with the EEJ (black curve) estimated using the pair of ground magnetometers in the Jicamarca meridian and is shown in the Figure 4 (bottom). The irregularity drift shows excellent correlation with the EEJ and with the IMF B_z quasiperiodic fluctuations shown in Figure 4 (top), implying a source and effect relationship between the IMF fluctuations and the vertical drift fluctuations at the equator.

4. Discussion and Conclusion

The interaction between the solar wind and the magnetosphere drives the region 1 (R1) and region 2 (R2) field-aligned current (FAC) systems and the associated magnetospheric plasma convection. The R1 and R2 FACs, in general, set up electric field that may generate current system at high latitude that has quasiperiodic fluctuation with very good one-to-one correlation with the IMF B_z variations. Since the magnetic effect of Pederson currents on the ground level is roughly equal in magnitude but opposite in sign to the magnetic effect of FAC, the magnetic disturbance observed at high-latitude ground level is due to Hall currents [e.g., *McPherron*, 1995]. Thus, the *DP* 2 fluctuations at high latitudes are due to the combined effect of Hall conductivity and the solar wind-driven convection electric field [e.g., *Clauer and Kamide*, 1985; *Kikuchi et al.*, 1996, 2000]. The *DP* 2 fluctuation then extends to the equatorial ionosphere almost instantaneously (see Figures 2 and 4) through the TM0 mode waves in the Earth-ionosphere waveguide [e.g., *Kikuchi et al.*, 2008]**.**

Figure 2 (second panel) shows the magnetic field at northern high and auroral latitudes (Thule (THL), Iqaluit (IQA), and Narsarsuaq (NAQ)) that mostly do not show clear correlation with IMF B_z fluctuations during the given time interval (09:00 UT–20:00 UT). The polar region (THL) magnetic variation was experiencing a deep magnetic bay during this time interval, which is expected as the station was in the nightside during this time interval in February. The strong magnetic bays were also observed at auroral latitudes (IQA) during 09:00–14:00 UT, which was in local morning toward local noon indicated by the blue vertical solid line. After 14:00 UT (i.e., when the station was moving to dayside) the *DP* 2 current dominates at IQA and shows coherent fluctuations with IMF B_z during 14:00–17:00 UT. The magnetic field variations at NAQ, of which its local noon is located at ~15:00 UT as indicated by green solid vertical line, do not show any significant magnetic bay; instead, it shows good correlation with IMF B_z during 14:00–19:00 UT. The midlatitude station (King Edward Point (KEP)) located on the dayside southern region mostly shows one-to-one correlation with the IMF B_z fluctuations. The comparison of magnetic fluctuations at different latitudes, such as at THL, IQA, NAQ, and KEP, shows the *DP* 2 fluctuations indeed decrease in magnitude as latitude decreases until it gets enhanced considerably (see Figure 2, third panel) due to the presence of Cowling effect at the dip equator.

The question is what makes the *DP* 2 current system fluctuates both at high and low latitudes coherently? It has been demonstrated that this could be due to the imbalance of *R*1 and *R*2 FAC current systems. By separating the R1 and R2 FACs from radar electric field measurements, using the combination of ground-based magnetometers and EISCAT radar data, *Kikuchi et al.* [2000] showed a significant decrease (increase) of EEJ at the geomagnetic equator when IMF B_z turns north (south) and when there is a steep decrease (increase) of R1 FACs and increase (decrease) of R2 FACs. The R2 FACs generally set up a transient electric field that is opposite in direction with that of R1 FACs and produce a shielding effect [e.g., *Kikuchi et al.*, 2008]. Similarly, when IMF B_z turns south (north) both the *DP* 2 current system and the EEJ at the equator get enhanced (decayed) or become eastward (westward), and irregularity drift at the equator turns upward (downward) as shown in Figures 2 and 3. The excellent time coincidence between the IMF B_z minimum points and EEJ peaks, as pointed out by the vertical dashed lines that pass through them, indicates that the EEJ enhanced (decayed) when IMF B_z turns south (north), which is consistent with the results reported in *Kikuchi et al.* [2000].

Thus, comparing Figures 2 and 3 the vertical dashed lines provide an excellent view that the periodic imbalance of R1 and R2 FAC systems causes the EEJ and thus the vertical drift velocity fluctuation at the equator. The fluctuating vertical drift, which controls the vertical motion of the ionosphere, in turn causes the *F* layer vertical height to fluctuate up (down) coherently with IMF B_z as shown in Figure 3. The positions of EEJ peaks (white curves) are directly correlated with ionosonde estimated ionospheric backscatter echo peaks as shown in Figure 3 (fourth panel). The fluctuating height of backscatter echo amplitude peaks, which often coincides with h_mF_2, is used to track the up and down movement of the ionospheric *F* layer. While the strong *F* region echoes show clearly visible up and down fluctuations of the *F* layer's virtual height during *DP* 2 fluctuations event on 16 February, the echoes detected by the same ionosonde during the time without *DP* 2 fluctuations event on 15 February do not show any up and down fluctuation. This clearly demonstrates how the *DP* 2 current fluctuation controls not only the electrodynamics but also the ionospheric *F* layer height. Similarly, the filtered VTECs from four different satellites (Figure 2, third panel) show almost coherent fluctuation with the EEJ and thus with IMF B_z. The time delay between the filtered VTEC as well as the ionospheric echo and EEJ peaks, in which the VTEC and ionospheric echo peaks appears about 20–30 min after EEJ peak time, is due to the duration of the vertical drift perturbation and that the ionospheric density peaks occur at the time when the layer stops moving upward or when the drift velocity reverse its direction. This clearly demonstrates that the magnetospheric origin quasiperiodic electric field can penetrate to the magnetosphere and drive *DP* 2 current fluctuations that extend to the lower latitude ionosphere and causes the EEJ and thus vertical drift at the equator to fluctuate and create significant effect on the equatorial density distribution by making the *F* layer moves up and down. Figure 4 (bottom) shows another example of the *DP* 2 current modulation of the drift velocity as it is demonstrated by the independently measured ionospheric irregularity drift (red curve) that fluctuates coherently with the EEJ as well as with *DP* 2 current and IMF B_z. Similar correlation between the magnetospheric origin electric field and the ground-based radar measured electric field during magnetic storm periods have been performed, mainly in the absence of *DP* 2 current fluctuation [e.g., *Kelley et al.*, 2003; *Huang et al.*, 2007; *Sobral et al.*, 1997]. However, for the first time, we report that the solar wind-magnetosphere-ionosphere interactions driven *DP* 2 current systems not only modulate ionospheric equatorial electrodynamics but also cause the ionospheric density distributions to fluctuate up and down.

It is worth mentioning about the small-scale fluctuation embedded in the large quasiperiodic EEJ variation, e.g., shown in between 16:45 and 17:50 UT in Figure 4. *Yizengaw et al.* [2013] reported that the ULF wave in the *Pc*5 range is the possible cause for the formation of those small-scale EEJ fluctuations that are predominantly visible in Figure 4 compared to that of Figure 2 where these fluctuations are visible only at the eastward peaks of EEJ.

In general, when the FACs are in continuous dynamic, they form significantly fluctuating *DP* 2 current systems that can easily penetrate to the equatorial region and modulate the equatorial electrodynamics that are responsible for the complicated nature of dayside ionospheric density height variations at the equator. Therefore, understanding of the *DP* 2 current systems, such as its source, condition of its penetration to the equatorial region, and the impact it can produce onto the ionospheric density distribution is very important to understand the physics of equatorial electrodynamics that govern the equatorial density distribution. Because its impact on the equatorial ionosphere is significant, it can greatly affect the communication and navigation systems.

Acknowledgments

This work has been partially supported by AFOSR (FA9550-12-1-0437 and FA9550-15-1-0399) and NSF (AGS145136 and AGS1450512) grants. The authors are indebted to the Jicamarca Radio Observatory and INTERMAGNET team for the magnetometer data resources they made available to the public. We also thank the Global Ionospheric Radio Observatory team for the ionosonde data. The solar wind data were obtained from the CDAWeb database.

References

Anderson, D., A. Anghel, J. Chau, and O. Veliz (2004), Daytime vertical $E \times B$ drift velocities inferred from ground-based magnetometer observations at low latitudes, *Space Weather*, *2*, S11001, doi:10.1029/2004SW000095.

Clauer, C. R., and Y. Kamide (1985), *DP*l and *DP*2 current systems for the March 22, 1979 substorms, *J. Geophys. Res.*, *90*, 1343–1354.

Huang, C. S., S. Sazykin, J. L. Chau, N. Maruyama, and M. C. Kelley (2007), Penetration electric fields: Efficiency and characteristic time scale, *J. Atmos. Sol. Terr. Phys.*, doi:10.1016/j.jastp.2006.08.06.

Kelley, M. C., J. J. Makela, J. L. Chau, and M. J. Nicolls (2003), Penetration of the solar wind electric field into the magnetosphere/ionosphere system, *Geophys. Res. Lett.*, *30*(4), 1158, doi:10.1029/2002GL016321.

Kikuchi, T., H. Lu¨hr, T. Kitamura, O. Saka, and K. Schlegel (1996), Direct penetration of the polar electric field to the equator during a DP2 event as detected by the auroral and equatorial magnetometer chains and the EISCAT radar, *J. Geophys. Res.*, *101*(A8), 17,161–17,173.

Kikuchi, T., H. Lühr, K. Schlegel, H. Tachihara, M. Shinohara, and T.-I. Kitamura (2000), Penetration of auroral electric fields to the equator during a substorm, *J. Geophys. Res.*, *105*, 23,251–23,261, doi:10.1029/2000JA900016.

Kikuchi, T., K. K. Hashimoto, and K. Nozaki (2008), Penetration of magnetospheric electric fields to the equator during a geomagnetic storm, *J. Geophys. Res.*, *113*, A06214, doi:10.1029/2007JA012628.

Love, J. J., and A. Chulliat (2003), An international network of magnetic observatories, *Eos*, *94*(42), 373–374.

McPherron, R. L. (1995), Magnetospheric dynamics, in *Introduction to Space Physics*, edited by M. G. Kivelson and C. T. Russell, pp. 400–458, Cambridge Univ. Press, New York.

Nishida, A. (1968), Coherence of geomagnetic *DP2* magnetic fluctuations with interplanetary magnetic variations, *J. Geophys. Res.*, *73*(17), 5549–5559.

Parker, E. N. (1967), Small-scale nonequilibrium of the magnetopause and its consequences, *J. Geophys. Res.*, *72*(17), 4365–4374.

Reinisch, B. W., and I. A. Galkin (2011), Global Ionospheric Radio Observatory (GIRO), *Earth Planet Space*, *63*(4), 377–381.

Sobral, J. H. A., M. A. Abdu, W. D. Gonzalez, B. T. Tsurutani, I. S. Batista, and A. L. C. Gonzalez (1997), Effects of intense storms and substorms on the equatorial ionosphere/thermosphere system in the American sector from ground-based and satellite data, *J. Geophys. Res.*, *102*(A7), 14,305–14,313.

Trivedi, N. B., D. G. Sibeck, E. Zesta, J. C. Santos, K. Yumoto, T. Kitamura, M. Shinohara, *and* S. L. G. Dutra (2002), Signatures of traveling convection vortices in ground magnetograms under the equatorial electrojet, *J. Geophys. Res.*, *107*, 1087, doi:10.1029/2001JA000153.

Valladares, C. E., and J. L. Chau (2012), The low-latitude ionosphere sensor network: Initial results, *Radio Sci.*, *47*, RS0L17, doi:10.1029/2011RS004978.

Yizengaw, E., and M. B. Moldwin (2009), African Meridian B-field Education and Research (AMBER) array, *Earth Moon Planet*, *104*(1), 237–246, doi:10.1007/s11038-008-9287-2.

Yizengaw, E., E. Zesta, C. M. Biouele, M. B. Moldwin, A. Boudouridis, B. Damtie, A. Mebrahtu, F. Anad, R. F. Pfaff, and M. Hartinger (2013), Observations of ULF wave related equatorial electrojet fluctuations, *J. Atmos. Sol. Terr. Phys.*, *103*, 157–168.

Yizengaw, E., M. B. Moldwin, E. Zesta, C. M. Biouele, B. Damtie, A. Mebrahtu, B. Rabiu, C. E. Valladares, and R. Stoneback (2014), The longitudinal variability of equatorial electrojet and vertical drift velocity in the African and American sectors, *Ann. Geophys.*, *32*, 231–238.